Scientific paper

A Highly Selective DNA Sensor Based on Graphene Oxide-Silk Fibroin Composite and AuNPs as a Probe Oligonucleotide Immobilization Platform

Ali Benvidi,[1,*] Zohreh Abbasi,[1] Marzieh Dehghan Tezerjani,[1] Maryam Banaei,[1] Hamid Reza Zare,[1] Hossein Molahosseini[2] and Shahriar Jahanbani[1]

[1] *Department of Chemistry, Faculty of Science, Yazd, Yazd, I. R. Iran*

[2] *Department of Textile Engineering, Isfahan University of Technology, Isfahan, Iran*

* *Corresponding author: E-mail: abenvidi@yazd.ac.ir, benvidi89@gmail.com*
Tel.: +98 353 812 2645; Fax: +98-353-8210644

Abstract

In this study, a simple and novel electrochemical biosensor based on a glassy carbon electrode (GCE) modified with a composite of graphene oxide (GO) – silk fibroin nanofibers (SF) and gold nanoparticles (MCH/ssDNA/AuNPs/SF/GO/GCE) was developed for detection of DNA sequences. The fabrication processes of electrochemical biosensor were characterized by scanning electron microscopy (SEM), FT-IR and electrochemical methods. Some experimental conditions such as immobilization time of probe DNA and MCH incubation time, time and temperature of hybridization were optimized. The designed biosensor revealed a wide linear range of $1.0 \times 10^{-16} - 1.0 \times 10^{-8}$ mol L^{-1} and a low detection limit (3.3×10^{-17} mol L^{-1}) for detection of BRCA1 5382 mutation by EIS technique. The designed biosensor revealed high selectivity for discrimination of the complementary (P1C) sequences from various non-complementary sequences of (P1nC1, P1nC2 and P1nC3). Also, the biosensor revealed a high reproducibility (RSD of 7.5% (n = 4)) and high stability (92% of its initial response after 8 days). So, the fabricated biosensor has a suitable potential to be applied for detection of breast cancer sequences in the initial stages of the cancer.

Keywords: DNA biosensor; immobilization; composite; silk nanofibers; graphene oxide nanosheets

1.Introduction

Breast cancer like other cancers initiates continuous process of aberrant chromosomal changes and consequently leads to damage to DNA.[1–3] As known, there are various clinical methods for detection of breast cancer such as mammography, magnetic resonance imaging (MRI) and breast biopsy tests.[4] Besides that up to now, lots of techniques such as surface plasmon resonance,[5,6] optical fiber,[7] quartz crystal microbalance,[8] micro cantilever and electrochemical methods have been developed for detection of cancers because the cancer detection in the initial stages is so important.[9–13] Most of the optical methods are indirect and need a labeling of target DNA. So, the electrochemical biosensors based on electrochemical techniques such as cyclic voltammetry (CV), differential pulse voltammetry (DPV) and electrochemical impedance spectroscopy (EIS) have been developed for detection of low

concentrations of DNA sequences.[14,15] Some great advantages of electrochemical biosensors compared to other types of biosensors are miniaturization, high sensitivity, low cost and fast detection. [16]

The immobilization step of the DNA probe on the electrode surface is important in determining the overall performance of an electrochemical DNA biosensor.[17] To have a good immobilization process, some materials such as polymer, ionic liquid and nanoparticles have been used as the biosensing interface.[18–21] Up to now, lots of nanoparticles have been applied for fabrication of biosensors due to some unique properties such as high surface-to-volume ratio, high conductivity and suitable biological compatibility.[22] Graphene is a one-atom-thick 2D carbon nanomaterial. Graphene oxide is a water dispersible version of graphene with oxygen-containing functional groups such as hydroxyl, carboxyl and epoxy groups.[23] Its nanosheets can adsorb single-stranded DNA (ssDNA) via

---

non-covalent p-stacking interactions between the hexagonal cells of graphene and the ring structure of nucleobases.[24] Graphene oxide (GO) has a key role in the construction of biosensors due to its unique characteristics such as good dispensability and simple surface functionality, high electronic, thermal and mechanical properties.[25–26] So, in the present work graphene oxide nanosheets were used for immobilization and hybridization processes of DNA strands at the electrode surface.

Another used nanomaterial in this study is silk nanofiber. Silk fibroin (SF) is a macromolecular protein with molecular weight about 350 kDa which can be extracted from silkworm cocoon. It is highly biocompatible and due to its porous structure allows the growing of cells, growth factors and the production of extracellular matrix (ECM) to enable communication between the cells. Fibroin is extremely versatile and can be processed in very different forms.[27–30] One of the most interesting polymers that could be combined with graphene is silk fibroin (SF). In addition to having an excellent and well known biocompatible properties,[31] fibroin is a protein with a secondary molecular structure in the form of a beta-sheet that combines well with graphene.[32,33] However, there are other configurations of fibroin scaffolds that could be improved after combination with graphene.

Recently, lots of electrochemical sensors based on various nanomaterials have been developed for detection of different targets.[34–39] For instance, S. M. Ghoreishi et al. designed an electrochemical method for determination of acetaminophen in different pharmaceutical forms using gold nanoparticles carbon paste electrode.[40] B. Bozzini group investigated the electro deposition of Co/CoO nanoparticles onto graphene for electrocatalysis of oxygen reduction reaction by a multi-technique approach.[41] Also, B. Mahltig and coworkers fabricated an antimicrobial agent by using the silver nanoparticles in SiO_2 microspheres.[42]

As known, voltammetric methods are simple, sensitive, selective and time-saving.[43] A DNA biosensor based on using electrochemical impedance spectroscopy (EIS) technique is a device that transduces changes in interfacial properties between the electrode and the electrolyte surface to an electrical signal. DNA biosensors based on EIS detection are label-free and it means that it is not necessary to use some labels such as fluorophore,[44–46] magnetic beads,[47] or an enzyme for detection of target.[48] Thus, some advantages of this kind of DNA biosensor are: low cost, simplicity, and ease of miniaturization. Also, when the differences in current are not significant in a low target concentration range, the EIS technique is more suitable than other electrochemical detection techniques.

Following our previous works,[4,49,50] in the present research an electrochemical biosensor for detection of BRCA1 sequences was designed. This biosensor is based on nano composite of graphene oxide – silk nanofibers and gold nanoparticles as a platform at the glassy carbon electrode (GCE). The fabrication processes of the designed sensor were followed by electrochemical impedance spectroscopy (EIS) and cyclic voltammetry (CV) methods. Under optimum conditions, the fabricated biosensor (MCH/ssDNA/AuNPs/SF/GO/GCE) revealed a wide linear range $(1.0 \times 10^{-16}$ to 1.0×10^{-8} mol $L^{-1})$ and a low detection limit of 3.3×10^{-17} mol L^{-1} using EIS method. The designed biosensor revealed a high selectivity for discrimination of complementary from different non-complementary sequences. Briefly, some advantages of MCH/ssDNA/AuNPs/SF/GO/GCE biosensor are: detecting DNA without using additional labels, easy preparation, possessing high selectivity, sensitivity, reproducibility and stability.

2. Experimental

2. 1. Reagents and Instruments

The used primers and probes were designed based on the breast cancer cells obtained from the Gen Bank database. 6-Mercapto-1-hexanol (MCH) was purchased from Aldrich. $HAuCl_4$ and all other chemicals were of analytical grade and obtained from Merck Company. All of the chemicals were used as received without further purification. The sequences of the used probe and complementary were as follows:

Probe sequence (P1):
5'-AAGCGAGCAAGAGAATTCCAG-3'
Complementary sequence (P1C):
5'- GTGAAAGTATCTAGCACTGCTGGAATTCT CTTGCTCGCTT-3'
Non-complementary sequence (P1nC1):
5'-TGTGAAAGTATCTAGCACTGTGGGAAT-TCTCTTGCTCGCT-3'
Non-complementary sequence (P1nC2):
5'-GAGAAACATCTGGGATA-3'
Non-complementary sequence (P1nC3):
5'-CACTTTATTTGGGATG-3

For electrochemical measurements an Autolab potentiostat/galvanostat model PGSTAT 302 N (Eco Chemic, Utrecht, Netherlands) and NOVA 1.7 software at laboratory temperature (25 ± 1 °C) were used. The used three-electrode system was composed of a modified glassy carbon electrode as working electrode, an Ag/AgCl (1.0 mol L^{-1} KCl) and a platinum wire as reference and auxiliary electrodes, respectively. A Metrohm model 691 pH/mV meter was applied for pH measurements. The graphene nanosheets were synthesized according to the procedure given in the literature.[25]

2. 2. Preparation of Nano Silk Fibroin

The natural silk fibers were purchased in a silk worm cocoon from Iran-Mazandaran area and then were cut into small pieces. To separate Srysyn gum, the small pieces of silk worm cocoon were boiled in the sodium carbonate solution (0/5% *w/w*) for 30 min two times. The resulting

fibers were rinsed with distilled water. The obtained silk fibroin was dried at room temperature and then dissolved in a solution containing calcium chloride/ethanol/water (molar ratio of 8/2/1) for 4 h at 60 °C. The resulting solution was purified using filtration process and dialyzed using a cellulose dialysis bag (12000) for 3 days at room temperature in the deionized water solution. The obtained solution as the diluted pure fibroin solution was dried at room temperature in a petri dish and the resulting film was converted to a powder. For preparation of fibroin nanoparticles, the physical method of ball mill grinding was applied for 12 h. The obtained FT-IR spectra of the resulting fibroin nanoparticles indicated a good agreement with other reported FT-IR of fibroin nanoparticles.[51]

2. 3. Preparation of MCH/ssDNA/SF/GO/GCE Biosensor

The fabrication processes of ssDNA/SF/GO/GCE biosensor include the steps as follows: at first, non-modified glassy carbon electrode (GCE) was polished by 0.05 μm alumina slurry to a mirror-like appearance, and then the mirror GCE was washed with anhydrous alcohol and water by ultrasonication for 30 min, respectively. At the second step, 20 μL of homogeneously dispersed solution of SF/GO (0.015/0.035 g/mL) nano composite was placed on the working electrode surface and dried under ambient conditions and this electrode was named SF/GO/GCE electrode. At the third step, gold nanoparticles (1.5 mmol L^{-1}) were deposited electrochemically on the surface of SF/GO/GCE electrode to prepare AuNPs/SF/GO/GCE (the applied experimental conditions: the potential range and the number of scans were –0.2 V to +0.9 V and 40, respectively). Fourth step contained dropping 20 μL of the DNA probe solution (1 μmol L^{-1}) at the surface of AuNPs/SF/GO/GCE for 12 h in a wet chamber to prepare ssDNA/AuNPs/SF/GO/GCE electrode. At the last step, the prepared electrode was immersed in a MCH (1 mol L^{-1}) solu-

tion as a blocker of surface to fill the bare areas of the ssDNA/AuNPs/SF/GO/GCE surface which have not been covered by DNA strands and remove nonspecific adsorption of DNA (MCH/ssDNA/AuNPs/SF/GO/GCE). After each step the electrode was rinsed with a buffer and the modification steps were followed by using EIS and CV techniques.

2. 4. The Solutions Preparation Procedure

The probe and complementary solutions provided from the Gen Bank database were dissolved in water and were kept frozen at –20 °C to form stock solution of primers (18.5 μmol L^{-1}). For preparation of solutions, deionized water (DI: 18 MΩ cm resistivity) was used. The solutions of DNA probe (1 μmol L^{-1}) and various concentration of complementary (1.0×10^{-16} mol L^{-1} to 1.0×10^{-8} mol L^{-1}) were prepared by sequential dilution of the stock solution of primers. Also, for preparation of SF/GO suspension, GO and SF (0.035 g, 0.015 g, respectively) was weighed and diluted with 1 mL of distilled water. Then, this suspension was sonicated for 1 h to prepare the solution of SF/GOI which was placed on the electrode surface. The probe DNA immobilization and hybridization were monitored in a solution containing [Fe(CN)$_6$]$^{3-/4-}$ (1:1) (1.0 mmol L^{-1}) and KCl (0.1 mol L^{-1}) mixture as the redox active probe (Scheme 1).

3. Results and Discussion
3. 1. Characterization of the Fabricated Biosensor

As shown in Fig. 1, the surface morphology of bare glassy carbon electrode (A), the modified glassy carbon with graphene oxide nanosheets (B), the silk nanofibers (C), nano composite of graphene oxide – silk fibroin (D),
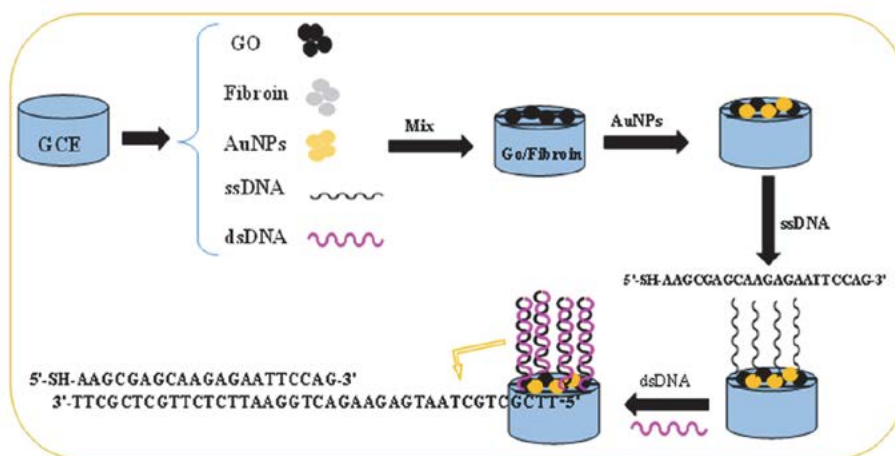
Scheme 1. The schematic diagram of the fabrication of MCH/ssDNA/AuNPs/SF/GO/GCE biosensor

the nano composite of graphene oxide – silk fibroin and nanoparticle AuNPs (E) was examined by scanning electron microscopy (SEM) technique. According to Fig. 1A, the bare glassy carbon electrode has a smooth surface area. Fig. 1B indicates the petal-like structure of graphene oxide nanosheets with a large surface area.[52] Fig. 1C shows the SEM of silk nanofibers compared with smooth surface of bare glassy carbon electrode.[53] Fig. 1D, shows the SEM of the modified glassy carbon electrode with nanosheets of

graphene oxide – silk nanofibers which can provide a suitable platform for DNA sensing by increasing the electrode surface area. As shown in Fig 1E, the SEM of the modified glassy carbon electrode with nanosheets of graphene oxide – silk nanofibers and gold nanoparticles (AuNPs) can provide a suitable platform for sensing of thiolated DNA strands via the formation of Au–S bond.

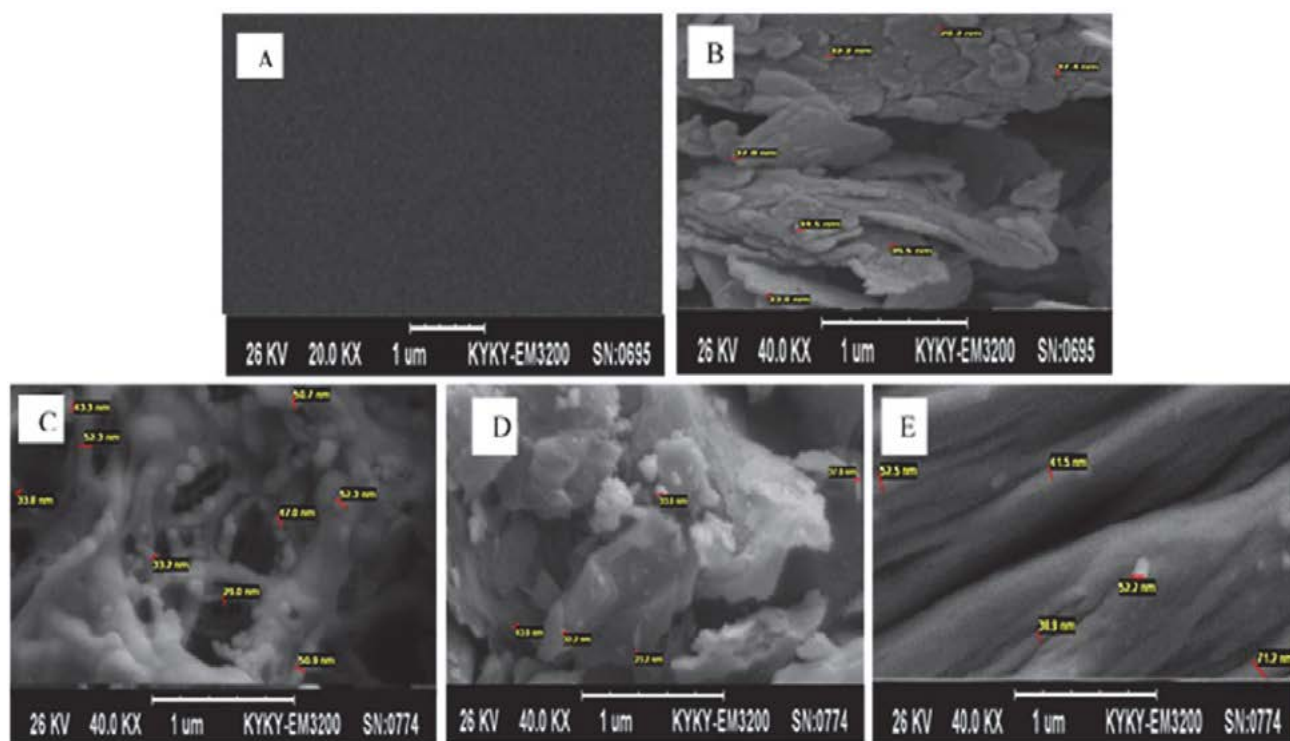For characterization of the used compounds for modification of the electrode surface the FT-IR spectros-

Figure 1. The SEM images of A) bare GCE, B) GO/GCE, C) SF/GCE, D) SF/GO/GCE and E) AuNPs/SF/GO/GCE electrodes
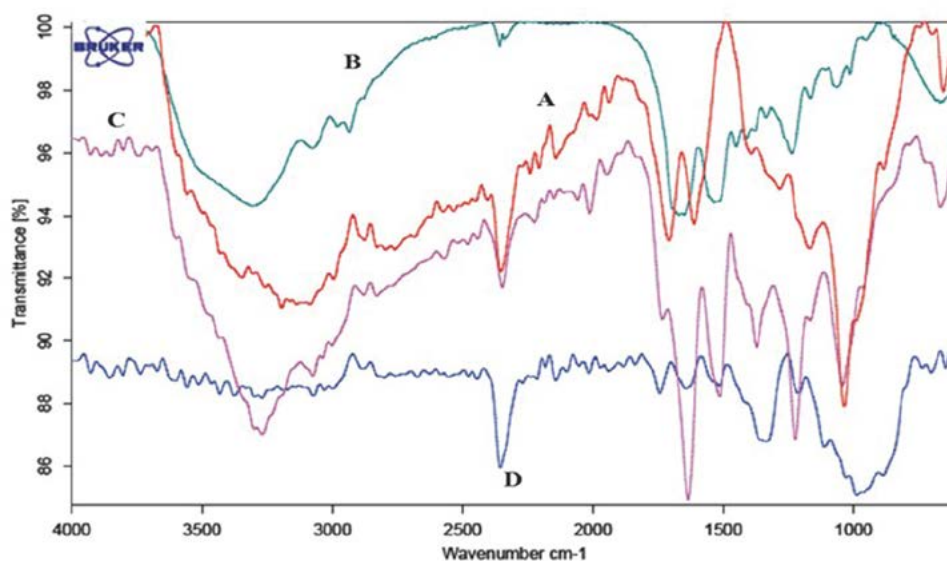

Figure 2. FT-IR spectrum of A) GO, B) SF, C) SF/GO composite and D) AuNPs/SF/GO.

copy technique was used. The FT-IR spectrum of graphene oxide reveals a C-O stretch at 1222 cm⁻¹, an O-H stretch at 3500–3300 cm⁻¹, and a C=O stretch at 1720–1690 cm⁻¹ [54] (Fig. 2A). Also, the FT-IR spectrum of silk nanofibers shows a hydrogen bond at 3300 cm⁻¹, a C-N stretch at 1444 cm⁻¹, C=O stretch at 1640–1620 cm⁻¹, a C-N stretch at 1230 cm⁻¹ (Fig. 2B). The FT-IR spectrum of SF/GO composite indicates the related peaks of both graphene oxide and silk fibroin in the SF/GO composite (Fig. 2C). After electro-deposition of gold nanoparticles on the SF/GO surface, a NH peak which is shifted to low energy is ob-

served in the SF/GO/AuNPs spectrum and this can be related to the interaction between the AuNPs and composite of SF/GO (see Fig. 2D). These observations denote that the modification of electrode surface was performed well.

Also, the modification processes of electrode were monitored with electrochemical techniques (cyclic voltammetry (CV) and impedance (EIS)). Fig. 3 indicates the obtained cyclic voltammograms of different electrodes in a solution containing $[Fe(CN)_6]^{3-/4-}$ (1.0 mol L⁻¹) at a scan rate of 100 mV/s. According to this figure, after introduction of SF/GO composite at the surface of bare glassy
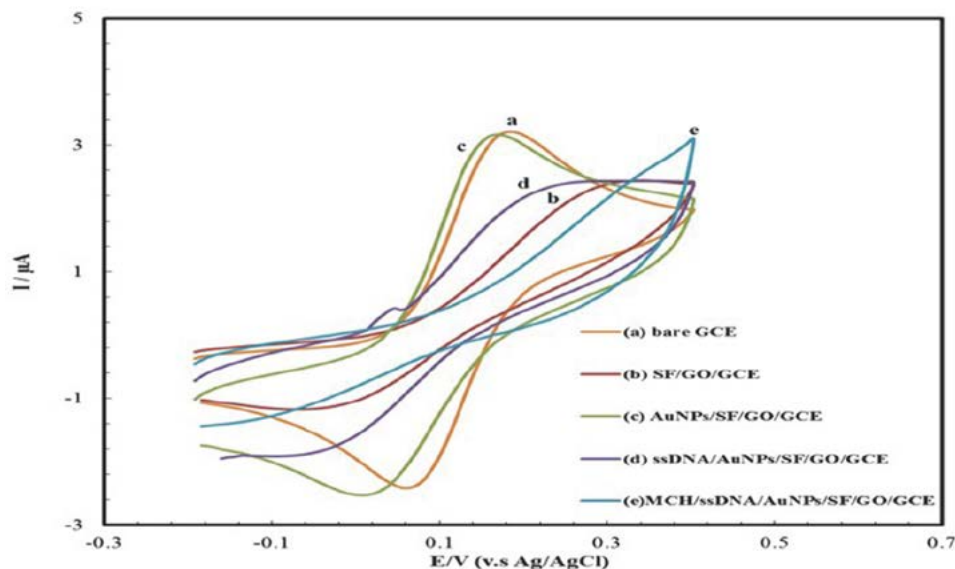
Figure 3. Cyclic voltammograms obtained for a 1.0 mmol L⁻¹ $[Fe(CN)_6]^{3-/4-}$ and 0.1 mol L⁻¹ KCl solution at the surfaces of (a) bare GCE, (b) SF/GO/GCE, (c) AuNPs/SF/GO/GCE, (d) ssDNA/ AuNPs/SF/GO/GCE, (e) MCH/ssDNA/AuNPs/SF/GO/GCE (CV condition: scan rate 50 mV s⁻¹).
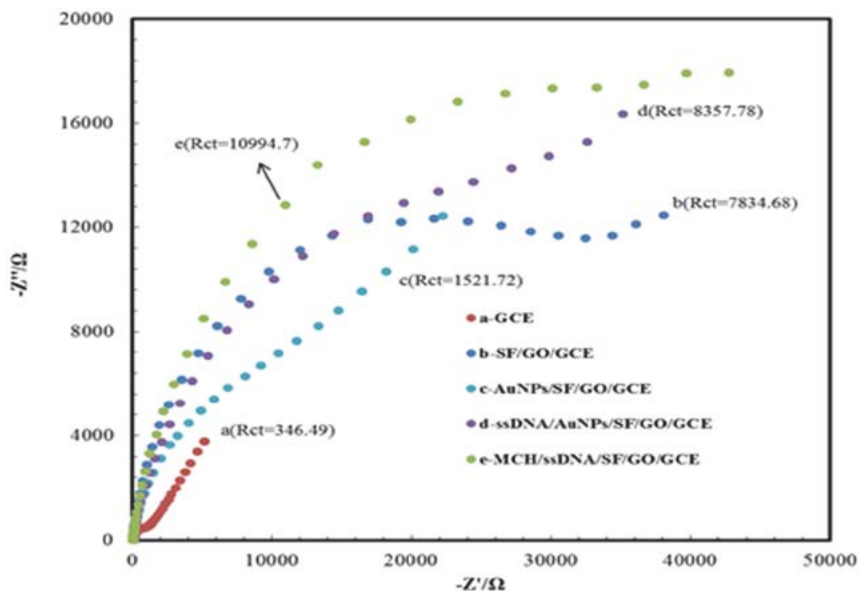
Figure 4. Electrochemical impedance spectroscopy (EIS) signals obtained for a 1.0 mmol L⁻¹ $[Fe(CN)_6]^{3-/4-}$ and 0.1 mol L⁻¹ KCl solution at the surfaces of (a) bare GCE, (b) GO/SF/GCE, (c) AuNPs/GO/SF/GCE, (d) ssDNA/ AuNPs/GO/SF/GCE, (e) MCH/ssDNA/AuNPs/GO/SF/GCE (EIS conditions: initial ac potential 0.20 V with an AC amplitude of 5 mV and frequency range 10 kHz to 0.1 Hz).

carbon electrode, the peak current (i_p) of SF/GO/GCE electrode is decreased compared with the CV response of the bare GCE (curves a and b). This observation can be related to the insulation of the SF layer.[55] By electrodeposition of gold nanoparticles on SF/GO/GCE surface, the peak current value is increased due to high conductivity of gold nanoparticles (curves b and c). It is noticeable that the existence of the gold nanoparticles at the modified electrode surface leads to more attachment of ss-DNA strands at the electrode surface (curve c). By immobilization of probe at the surface of the AuNPs/SF/GO/GCE, the peak current is decreased due to the repellence of $[Fe(CN)_6]^{3-/4-}$ by the negatively charged phosphate backbone of probe DNA and also the saturation of the electrode surface by probe DNA to prevent $[Fe(CN)_6]^{3-/4-}$ ions from reaching the electrode surface (curve c and d). After blocking the electrode surface by MCH (1.0 mmol L^{-1}) as a blocker surface at the ss-DNA/AuNPs/SF/GO/GCE, the peak current is decreased (curve e).

In addition, the fabrication process of MCH/ssDNA/AuNPs/SF/GO/GCE was followed with EIS method (Fig. 4). The modification of the bare glassy carbon electrode surface with SF/GO composite causes an increase of the semicircle diameter (R_{ct}) compared to bare GCE (curves a, b). After electrodeposition of gold nanoparticles on the modified electrode surface with SF/GO composite, the val-

ue of R_{ct} is decreased due to the high conductivity of gold nanoparticles (curves b and c). By immobilization of the ss-DNA probe at the AuNPs/SF/GO/GCE surface, R_{ct} value is increased (curve d). Finally, using MCH solution as a blocker agent of electrode surface (ssDNA/AuNPs/SF/GO/GCE) leads to an increase in the value of R_{ct} (curve e). These results reveal that the fabrication process of MCH/ssDNA/AuNPs/SF/GO/GCE biosensor is performed well.

3. 2. Optimization of Experimental Conditions

3. 2. 1. Optimization of the Percentages of GO in the SF/GO Composite, Immobilization Time of Probe DNA and MCH Incubation Time

For increasing the sensitivity of the designed electrochemical sensor (ssDNA/SF/GO/GCE), some experimental parameters such as the percentages of GO in the SF/GO composite was optimized. The influence of the GO percentage in SF/GO composite was examined in the range of 30 to 90% *w/w*. The results revealed that the ΔR_{ct} values are increased by increasing the percentages of GO in the composite up to 70% *w/w* and after that, by increasing the percentages of GO the ΔR_{ct} values are nearly constant. So, the
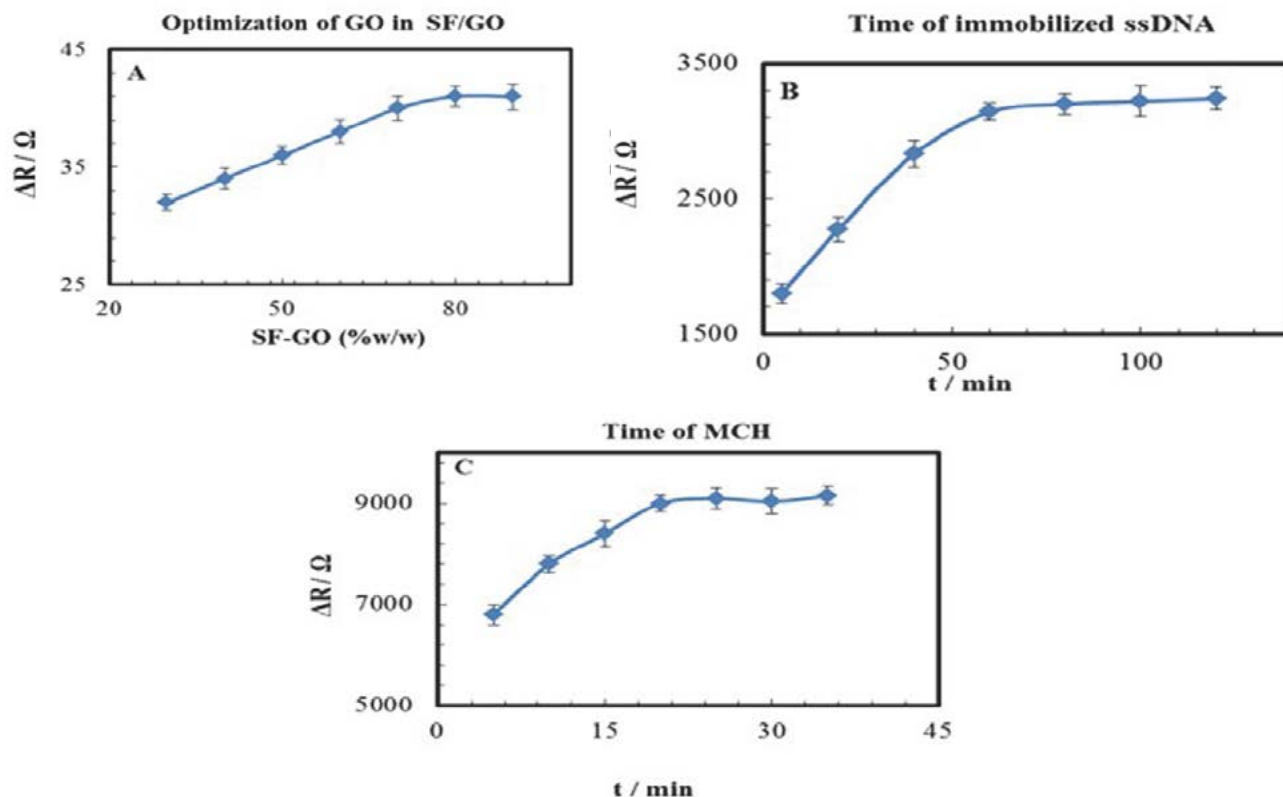
Figure 5. Optimization of operating conditions in a solution containing 0.5 mmol L^{-1} $[Fe(CN)_6]^{3-/4-}$ and 0.1 mol L^{-1} KCl (the number of independent experiments n = 3): (A) the percentages of GO in the composite of SF/GO, (B) the effect of immobilization time of ssDNA (1.0×10^{-6} mol L^{-1}), (C) the effect of MCH incubation time.

GO percentage of 70% *w/w* was chosen as the optimum percentage value of GO in the SF/GO composite (see Fig. 5A).

For investigation of immobilization time of probe DNA, 20 µL of the probe DNA solution (1×10^{-6} mol L^{-1}) was introduced at the electrode surface from 5 min to 2 h. According to Fig. 5B, it is observed that by increasing time, ΔR_{ct} values are increased until 1 h and then, ΔR_{ct} values remain constant. So, an immobilization time of 1 h was selected as an optimum immobilization time of probe DNA for further experiments (Fig. 5B). Also, for enhancement of selectivity and sensitivity of the proposed DNA biosensor, the MCH incubation time was investigated. As mentioned before, MCH incubation has an important role to remove the nonspecifically adsorbed probe molecules from the electrode surface. So, ssDNA/AuNPs/SF/GO/GCE electrode was immersed in a solution of MCH (1 mol L^{-1}) for a specific time. MCH can bind to the electrode surface and consequently prevents the absorption of complementary DNA sequences to the electrode surface. After incubation of the fabricated sensor in a solution containing MCH (1 mol L^{-1}), the ΔR_{ct} values are increased until 20 min and then the ΔR_{ct} values are constant (Fig. 5C). Based on these observations, the optimum time of 20 min was selected for the incubation of MCH.

3. 2. 2. Optimization of Time and Temperature of Hybridization

Other parameters which were optimized in this research are the effects of time and temperature of hybridization. The effect of hybridization time was investigated over the range of 5 min to 60 min while temperature and ssDNA concentration were kept constant at 25 °C and 1.0×10^{-16} mol L^{-1}, respectively. According to obtained results in Fig. 6A, 40 min was selected as the optimum hybridization time for further experiments.

Also, due to the importance of the temperature of hybridization for hybridization reaction, the temperature of hybridization was optimized. Hybridization temperature was changed from 25 to 65 °C while keeping hybridization time and complementary concentration constant at 50 min and 1.0×10^{-16} mol L^{-1}, respectively. As shown in Fig. 6B, the ΔR_{ct} values are constant up to 35 °C and then rapidly decrease by increasing the temperature due to replacement of some molecules from the electrode surface. Thus, the temperature of 25 °C was selected as the optimum hybridization temperature.

### 3. 3. Investigation of Sensitivity of MCH/ ssDNA/AuNPs/SF/GO/GCE Biosensor

The sensitivity of MCH/ssDNA/AuNPs/SF/GO/GCE biosensor was investigated by electrochemical impedance spectroscopy (EIS) technique. Fig. 7 reveals the impedance signals of the fabricated biosensor versus various concentrations of complementary target DNA sequences. Inset (A) of Fig. 7 reveals that the ΔR_{ct} values versus various target concentrations have a linear relationship in the range from 1.0×10^{-16} mol L^{-1} to 1.0×10^{-8} mol L^{-1} with a regression equation of $\Delta R_{ct} = 698.6 \log C$ (mol L^{-1}) + 18480 (R = 0.9914). The detection limit based on $3s_{bl}$ (where the s_{bl} was the standard deviation of 10 replicate measurements of MCH/ssDNA/AuNPs/SF/GO/GCE in [Fe(CN)$_6$]$^{3-/4-}$] solution) was calculated to be 3.3×10^{-17} mol L^{-1}. Inset (B) of this figure indicates the used Randles equivalent circuit in this study while R$_s$ is the electrolyte (1.0 mmol L^{-1} [Fe(CN)$_6$]$^{3-/4-}$ and 0.1 mol L^{-1} KCl) resistance, CPE is constant phase element, W$_{01}$ is Warburg impedance resulting from the diffusion of ions and R$_{ct}$ is the electron transfer resistance. Due to the significant influence of electron transfer process between [Fe(CN)$_6$]$^{3-/4-}$ and electrode surface during the modification and hybridization processes, the R$_{ct}$ values are used. The obtained
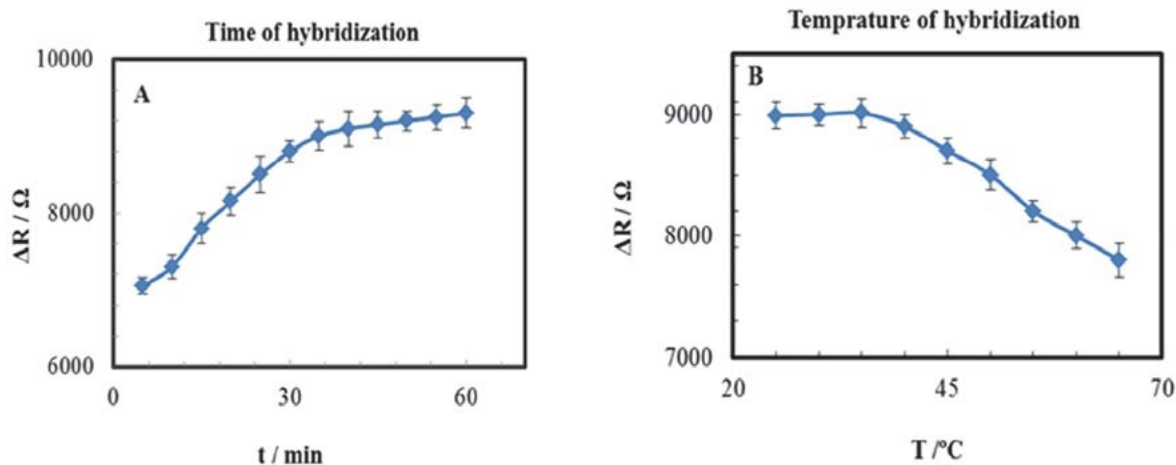
Figure 6. Optimization of operating conditions in a solution containing [Fe(CN)$_6$]$^{3-/4-}$ (0.5 mmol L^{-1}) and KCl (0.1 mol L^{-1}) and the number of independent experiments is 3 (n=3): (A) the influence of target DNA (1×10^{-12} mol L^{-1}) interaction time and (B) the effect of hybridization temperature.

results reveal that using the nano composite of GO and SF in the structure of MCH/ssDNA/AuNPs/SF/GO/GCE biosensor leads to increasing the sensitivity of the designed biosensor due to the unique properties of GO such as possessing lots of carboxylic acid groups, increasing the surface area, good biocompatibility and electron mobility at room temperature[56] and also some specific properties of SF like tensile strength and elasticity, good thermal stability, hygroscopicity, microbial resistance and biocompatibility.[57] Also, Table 1 reveals the comparison of some charac-

teristics of ssDNA/SF/GO/GCE biosensor with some other reported electrodes.[58–62] According to Table 1, the obtained detection limit and linear range in this work are better than in other works. It is noticeable that the ssDNA/SF/GO/GCE biosensor has a good sensitivity for detection of BRCA 1 sequences but it has some disadvantages like: (i) EIS is used for DNA detection which is so sensitive towards the electrode surface changes but its selectivity is lower than in some other electrochemical techniques such as differential pulse voltammetry; (ii) the proposed meth-
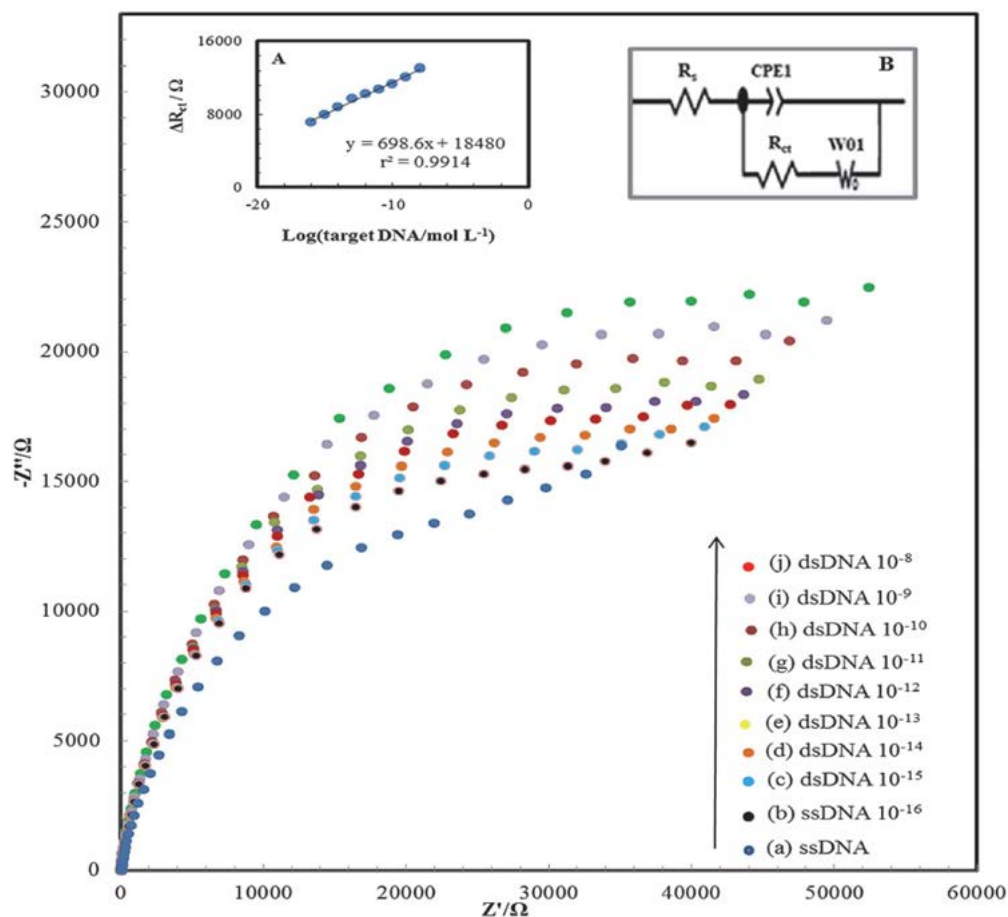
Figure 7. The obtained EIS signals for various concentrations of complementary DNA. Inset A: the applied Randles equivalent circuit, Inset B: the dependence of ΔR_{ct} versus the logC of target (DNA).

Table 1. Comparison of analytical performances of the MCH/ssDNA/AuNPs/SF/GO/GCE biosensor with several reported electrochemical DNA sensors for detection of breast cancer.

Electrode	Detection technique	Linear range (mol L^{-1})	Detection limit (mol L^{-1})	Ref.
MWCNTs/GCE	DPV	$0.1 \times 10^{-9} - 1000 \times 10^{-9}$	5.0×10^{-11}	[58]
GCE	DPV	$2 \times 10^{-10} - 5 \times 10^{-8}$	1.0×10^{-10}	[59]
DNA/PICA/GCE	EIS	$1 \times 10^{-9} - 2 \times 10^{-8}$	5×10^{-10}	[60]
Polypyrrole/DNA/MWCNT	CV	$3.3 \times 10^{-9} - 1.06 \times 10^{-8}$	1.0×10^{-9}	[61]
PPy/DNA/CNT/GCE	DPV	$1.0 \times 10^{-10} - 1.0 \times 10^{-8}$	8.5×10^{-11}	[62]
MCH/ssDNA/AuNPs/SF/GO/GCE	EIS	$1.0 \times 10^{-16} - 1.0 \times 10^{-8}$	3.3×10^{-17}	This work

od is quite time consuming; and (iii) it was not applied to a real sample although we believe that the fabricated biosensor has a good potential for detection of breast cancer in the near future.

3. 4. The Selectivity Investigation of the Fabricated Biosensor

As known, the selectivity is explained as the recognition of differences between the target DNA sequences from others. For investigation of the selectivity of the ssDNA/SF/GO/GCE biosensor, the fabricated biosensor was hybridized with complementary P1C and different non-complementary sequences of P1nC1, P1nC2 and P1nC3. The obtained results are shown in Fig. 8. According to this figure, ssDNA/SF/GO/GCE biosensor reveals different EIS signals after hybridization with 1.0×10^{-13} mol L^{-1} of complementary P1C (6400 kΩ) and 1.0×10^{-13} mol L^{-1} of various non-complementary DNA sequences P1nC1, P1nC2 and P1nC3 (690, 600 and 580 kΩ, respectively). These observations indicate that the fabricated biosensor has a high selectivity and also it can be suggested that the designed biosensor will be applied in the future for real samples.
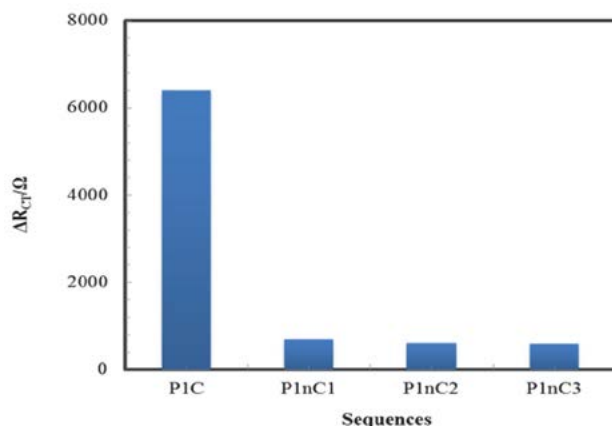
Figure 8. The specificity test using the MCH/ssDNA/AuNPs/SF/GO/GCE biosensor responses to different targets of complementary (P1C) and non-complementary (P1nC1, P1nC2 and P1nC3) sequences.

3. 5. Reproducibility and Stability of the MCH/ssDNA/AuNPs/SF/GO/GCE Biosensor

The reproducibility and stability of MCH/ssDNA/AuNPs/SF/GO/GCE biosensor were examined. For reproducibility investigation of the designed biosensor, three ssDNA/SF/GO/GCE electrodes were fabricated and then hybridized with target DNA (1.0×10^{-13} mol L^{-1}). It is noticeable that independent DNA sensors were prepared in the similar conditions like suspension concentration of SF/GO composite, ssDNA immobilization and hybridization

of complementary sequences. The obtained results revealed a relative standard deviation (RSD) of 7.5% (n = 4) for ΔR where $\Delta R = R_{final} - R_{initial}$, and R_{final} is EIS response after hybridization and $R_{initial}$ is EIS signal before hybridization. Thus, the obtained results reveal a satisfactory reproducibility of this electrochemical biosensor. The stability of the MCH/ssDNA/AuNPs/SF/GO/GCE biosensor was also investigated during 8 days. The proposed biosensor was stored in a 0.1 mol L^{-1} phosphate buffer solution (pH 7.4) in the refrigerator at 4 °C and after 8 days the response of the ssDNA/SF/GO/GCE biosensor retained about 92% of its initial response. These observations prove the high stability of the fabricated DNA sensor.

4. Conclusions

In this paper, a DNA electrochemical biosensor based on graphene oxide nanosheets – silk fibroin composite as probe oligonucleotide immobilization platform was designed for breast cancer sequences detection. The modification processes of electrode were followed by scanning electron microscopy (SEM), FT-IR and electrochemical techniques of cyclic voltammetry (CV) and impedance (EIS). Some experimental parameters of the designed biosensor like the percentages of GO in the SF/GO composite, immobilization time of probe DNA and MCH incubation time, time and temperature of hybridization processes were optimized. Under optimum conditions, this electrochemical biosensor revealed a suitable dynamic range (1.0×10^{-16} mol L^{-1} to 1.0×10^{-8} mol L^{-1}) and a low detection limit (3.3×10^{-17} mol L^{-1}) for target DNA by EIS technique. The obtained results revealed high sensitivity of the fabricated biosensor. This method was successful in detection of BRCA 1 sequences containing complementary P1C sequences and various non-complementary sequences of P1nC1, P1nC2 and P1nC3. Briefly, this designed biosensor possesses some advantages such as suitable selectivity and sensitivity, high reproducibility and being not expensive. This biosensor like other designed sensors has some disadvantages such as being quite time consuming and was not applied to real samples. We hope that our explorations may present a basis for further advancement in modified electrochemical DNA biosensors applyed to various science fields.

5. Acknowledgements

6. References

1. R. Sager, *Cancer Res.* **1986**, *46*, 1573–1580.
2. J. H. Ray and J. German, *Chromosome mutation and neoplasia*, **1983**, 135–167.

3. J. D. Rowley, *Chromosomes and cancer: from molecules to man*, Academic Pr, 1983.

4. A. Benvidi, N. Rajabzadeh, M. Mazloum-Ardakani, M. M. Heidari and A. Mulchandani, *Biosens. Bioelectron.* **2014**, *58*, 145–152. **DOI:**10.1016/j.bios.2014.01.053

5. S. Maheswaran, L. V. Sequist, S. Nagrath, L. Ulkus, B. Brannigan, C. V. Collura, E. Inserra, S. Diederichs, A. J. Iafrate and D. W. Bell, *N Engl. J. Med.* **2008**, *359*, 366–377. **DOI:**10.1056/NEJMoa0800668

6. Y.-T. Long, C.-Z. Li, T. C. Sutherland, H.-B. Kraatz and J. S. Lee, *Anal. chem.* **2004**, *76*, 4059–4065. **DOI:**10.1021/ac049482d

7. F. J. Steemers, J. A. Ferguson and D. R. Walt, *Nat. Biotechnol.* **2000**, *18*, 91–94. **DOI:**10.1038/72006

8. M. Duman, R. Saber and E. Pişkin, *Biosens. Bioelectron.* **2003**, *18*, 1355–1363. **DOI:**10.1016/S0956-5663(03)00087-3

9. J. Wang and A. J. Bard, *Anal. chem.* **2001**, *73*, 2207–2212. **DOI:**10.1021/ac001344a

10. L. A. Thompson, J. Kowalik, M. Josowicz and J. Janata, *J. Am. Chem. Soc.* **2003**, *125*, 324–325. **DOI:**10.1021/ja027929z

11. H. Korri-Youssoufi and A. Yassar, *Biomacromolecules*, **2001**, *2*, 58–64. **DOI:**10.1021/bm0000440

12. J. Wang, *Chem. Eur. J.* **1999**, *5*, 1681–1685. **DOI:**10.1002/(SICI)1521-3765(19990604)5:6<1681::AID-CHEM1681>3.0.CO;2-U

13. K. Kerman, M. Kobayashi and E. Tamiya, *Meas. Sci. Technol.* **2003**, *15*, R1. **DOI:**10.1088/0957-0233/15/2/R01

14. A. Benvidi, M. D. Tezerjani, A. D. Firouzabadi, M. Mazloum-Ardakani and S. M. Moshtaghioun, *JICS.* **2016**, *13*, 2135–2142. **DOI:**10.1007/s13738-016-0931-x

15. H. Karimi-Maleh, F. Tahernejad-Javazmi, N. Atar, M. L. t. Yola, V. K. Gupta and A. A. Ensafi, *Ind. Eng. Chem. Res.* **2015**, *54*, 3634–3639. **DOI:**10.1021/ie504438z

16. C. Tlili, H. Korri-Youssoufi, L. Ponsonnet, C. Martelet and N. J. Jaffrezic-Renault, *Talanta* **2005**, *68*, 131–137. **DOI:**10.1016/j.talanta.2005.04.069

17. S. Cheraghi, M. A. Taher, H. Karimi-Maleh, E. Faghih-Mirzaei, New J. Chem. **2017**, *41*, 4985–4989. **DOI:**10.1039/C7NJ00609H

18. A. Benvidi, M. D. Tezerjani, S. M. Moshtaghiun and M. Mazloum-Ardakani, *Microchim. Acta* **2016**, *183*, 1797–1804. **DOI:**10.1007/s00604-016-1810-y

19. N. Zhu, Z. Chang, P. He and Y. Fang, *Electrochim. Acta* **2006**, *51*, 3758–3762. **DOI:**10.1016/j.electacta.2005.10.038

20. Z. Liu, B. Zhao, Y. Shi, C. Guo, H. Yang and Z. Li, *Talanta* **2010**, *81*, 1650–1654. **DOI:**10.1016/j.talanta.2010.03.019

21. M. O'hare and E. Nice, *J. Chromatogr. A* **1979**, *171*, 209–226. **DOI:**10.1016/S0021-9673(01)95300-2

22. R. Vaidyanathan, S. Dey, L. G. Carrascosa, M. J. Shiddiky, M. Trau, *Biomicrofluidics*, **2015**, *9*, 061501. **DOI:**10.1063/1.4936300

23. Y.-T. Cheng, C.-C. Pun, C.-Y. Tsai and P.-H. Chen, *Sens. Actuators, B* **2005**, *109*, 249–255. **DOI:**10.1016/j.snb.2004.12.072

24. K. S. Novoselov, A. K. Geim, S. V. Morozov, D. Jiang, Y. Zhang, S. V. Dubonos, I. V. Grigorieva and A. A. Firsov, *science* **2004**, *306*, 666–669.

25. D. C. Marcano, D. V. Kosynkin, J. M. Berlin, A. Sinitskii, Z. Sun, A. Slesarev, L. B. Alemany, W. Lu and J. M. Tour, *ACS nano*, **2010**, *4*, 4806–4814. **DOI:**10.1021/nn1006368

26. J. Lee, Y.-K. Kim and D.-H. Min, *Anal. chem.* **2011**, *83*, 8906–8912. **DOI:**10.1021/ac201298r

27. Y. Yang, X. Chen, F. Ding, P. Zhang, J. Liu and X. Gu, *Biomaterials*, **2007**, *28*, 1643–1652. **DOI:**10.1016/j.biomaterials.2006.12.004

28. L. Soffer, X. Wang, X. Zhang, J. Kluge, L. Dorfmann, D. L. Kaplan and G. Leisk, *J. Biomater. Sci., Polym. Ed.* **2008**, *19*, 653–664. **DOI:**10.1163/156856208784089607

29. M. K. Hota, M. K. Bera, B. Kundu, S. C. Kundu, C. K. Maiti, *Adv. Funct. Mater.* **2012**, *22*, 4493–4499. **DOI:**10.1002/adfm.201200073

30. S. Aznar-Cervantes, M. I. Roca, J. G. Martinez, L. Meseguer-Olmo, J. L. Cenis, J. M. Moraleda and T. F. Otero, *Bioelectrochemistry*, **2012**, *85*, 36–43. **DOI:**10.1016/j.bioelechem.2011.11.008

31. S. Aznar-Cervantes, J. G. Martínez, A. Bernabeu-Esclapez, A. A. Lozano-Pérez, L. Meseguer-Olmo, T. F. Otero and J. L. Cenis, *Bioelectrochemistry*, **2016**, *108*, 36–45. **DOI:**10.1016/j.bioelechem.2015.12.003

32. K. Hu, M. K. Gupta, D. D. Kulkarni and V. V. Tsukruk, *Adv. Mater* **2013**, *25*, 2301–2307. **DOI:**10.1002/adma.201300179

33. S. Ling, C. Li, J. Adamcik, S. Wang, Z. Shao, X. Chen and R. Mezzenga, *ACS Macro Letters*, **2014**, *3*, 146–152. **DOI:**10.1021/mz400639y

34. H. Karimi-Maleh, M. Hatami, R. Moradi, M. A. Khalilzadeh, S. Amiri, H. Sadeghifar, *Microchim. Acta* **2016**, *183*, 2957–2964. **DOI:**10.1007/s00604-016-1946-9

35. H. Karimi-Maleh, A. F. Shojaei, K. Tabatabaeian, F. Karimi, Sh. Shakeri, R. Moradi, *Biosens. Bioelectron.* **2016**, *86*, 879–884. **DOI:**10.1016/j.bios.2016.07.086

36. H. Karimi-Maleh, F. Amini, A. Akbari, M. Shojaei, *J. Colloid Interf. Sci.* **2017**, *495*, 61–67. **DOI:**10.1016/j.jcis.2017.01.119

37. S. Cheraghi, M. A. Taher, H. Karimi-Maleh. *J. Food Compost. Anal. J.* **2017**, *62*, 254–259. **DOI:**10.1016/j.jfca.2017.06.006

38. S. Cheraghi, M. A. Taher, H. Karimi-Maleh. *Appl. Ssrf. Sci.* **2017**, *420*, 882–885. **DOI:**10.1016/j.apsusc.2017.05.218

39. M. Shabani-Nooshabadi, M. Roostaee, H. Karimi-Maleh. *J. Iran. Chem. Soc.* **2017**, *14*, 955–961. **DOI:**10.1007/s13738-016-1045-1

40. S. M. Ghoreishi, M. Behpour, S. Sadeghzadeh and M. Golestaneh, *Acta Chim. Slov.* **2011**, *58*, 69–74.

41. B. Bozzini, P. Bocchetta, A. Gianoncelli, C. Mele and M. Kiskinova, *Acta Chim. Slov.* **2014**, *61*, 263–271.

42. B. Mahltig, H. Haufe, K. Muschter, A. Fischer, Y. H. Kim, E. Gutmann, M. Reibold, D. C. Meyer, T. Textor and C. W. Kim, *Acta Chim. Slov.* **2010**, *57*, 451–457.

43. M. Kaushik, S. Mahendru, M. Kumar, S. Chaudhary and S. Kukreti, *Advanced Techniques in Biology & Medicine*, **2016**, 1–6.

44. J. Liu, Z. Cao and Y. Lu, *Chem. Rev.* **2009**, *109*, 1948–1998. **DOI:**10.1021/cr030183i

45. J. N. Wilson, Y. N. Teo and E. T. Kool, *J. Am. Chem. Soc.* **2007**, *129*, 15426–15427. **DOI:**10.1021/ja075968a

46. J.-Y. Park and S.-M. Park, *Sensors*, **2009**, *9*, 9513–9532. **DOI:**10.3390/s91209513

47. D. R. Baselt, G. U. Lee, M. Natesan, S. W. Metzger, P. E. Sheehan, R. J. Colton, *Biosens. Bioelectron.* **1998**, *13*, 731–739. **DOI:**10.1016/S0956-5663(98)00037-2

48. S.-y. Niu, Q.-y. Li, R. Ren and S.-s. Zhang, *Biosens. Bioelectron.* **2009**, *24*, 2943–2946. **DOI:**10.1016/j.bios.2009.02.022

49. A. Benvidi, N. Rajabzadeh, M. Mazloum-Ardakani and M. M. Heidari, *Sens. Actuators, B* **2015**, *207*, 673–682. **DOI:**10.1016/j.snb.2014.10.043

50. M. D. Tezerjani, A. Benvidi, M. Rezaeinasab, S. Jahanbani, S. M. Moshtaghioun, M. Youssefi and K. Zarrini, *Anal. Methods*, **2016**, *8*, 7507–7515. **DOI:**10.1039/C6AY01524G

51. C. Zhao, J. Yao, H. Masuda, R. Kishore and T. Asakura, *Biopolymers*, **2003**, *69*, 253–259. **DOI:**10.1002/bip.10350

52. R. Jain, A. Sinha and A. L. Khan, *Mater. Sci. Eng., C* **2016**, *65*, 205–214. **DOI:**10.1016/j.msec.2016.03.115

53. B. Kundu, R. Rajkhowa, S. C. Kundu and X. Wang, *Adv. Drug Deliv. Rev.* **2013**, *65*, 457–470. **DOI:**10.1016/j.addr.2012.09.043

54. J. R. Lomeda, C. D. Doyle, D. V. Kosynkin, W.-F. Hwang and J. M. Tour, *J. Am. Chem. Soc.* **2008**, *130*, 16201–16206. **DOI:**10.1021/ja806499w

55. H. Yin, Y. Zhou, J. Xu, S. Ai, L. Cui and L. Zhu, *Anal. Chim. Acta* **2010**, *659*, 144–150. **DOI:**10.1016/j.aca.2009.11.051

56. A. Benvidi, A. D. Firouzabadi, S. M. Moshtaghiun, M. Mazloum-Ardakani and M. D. Tezerjani, *Anal. Biochem.* **2015**, *484*, 24–30. **DOI:**10.1016/j.ab.2015.05.009

57. Y.-Q. Zhang, *Biotechnol. Adv.* **1998**, *16*, 961–971. **DOI:**10.1016/S0734-9750(98)00012-3

58. Y. Xu, Y. Jiang, H. Cai, P.-G. He and Y.-Z. Fang, *Anal. Chim. Acta*, **2004**, *516*, 19–27. **DOI:**10.1016/j.aca.2004.04.013

59. H. Cai, X. Cao, Y. Jiang, P. He and Y. Fang, *Anal. Bioanal. Chem.* **2003**, *375*, 287–293. **DOI:**10.1007/s00216-002-1652-9

60. X. Xu, X. Weng, A. Liu, Q. Lin, C. Wang, W. Chen and X. Lin, *Anal. Bioanal. Chem.*, **2013**, *405*, 3097–3103. **DOI:**10.1007/s00216-013-6715-6

61. X. Li, J. Xia and S. Zhang, *Ana. chim. acta*, **2008**, *622*, 104–110.

62. H. Qi, X. Li, P. Chen and C. Zhang, *Talanta* **2007**, *72*, 1030–1035. **DOI:**10.1016/j.talanta.2006.12.032

Povzetek

V tej študiji smo razvili preprost nov elektrokemični biosenzor za detekcijo DNA sekvenc, osnovan na steklasti ogljikovi elektrodi (GCE), modificirani s kompozitom iz grafenovega oksida (GO) in nanovlaken svilenega fibroina (SF) ter z zlatimi nanodelci (MCH/ssDNA/AuNPs/SF/GO/GCE). Procese izdelave elektrokemičnega biosenzorja smo spremljali z vrstično elektronsko mikroskopijo (SEM), FT-IR in z elektrokemičnimi metodami. Optimizirali smo nekatere eksperimentalne pogoje, kot so: čas imobilizacije DNA in čas inkubacije z MCH, čas in temperatura hibridizacije. Pripravljeni biosenzor je izkazal široko linearno območje od $1,0 \times 10^{-16}$ do $1,0 \times 10^{-8}$ mol L^{-1} ter nizko mejo zaznave ($3,3 \times 10^{-17}$ mol L^{-1}) za detekcijo mutacije BRCA1 5382 s tehniko EIS. Izkazal je tudi visoko selektivnost za ločevanje med komplementarnimi (P1C) sekvencami in različnimi nekomplementarnimi sekvencami (P1nC1, P1nC2 in P1nC3). Biosenzor je imel tudi visoko obnovljivost (RSD 7,5% (n = 4)) in visoko stabilnost (92% začetnega odziva po 8 dnevih). Pripravljeni biosenzor ima torej ustrezen potencial za uporabo pri odkrivanju sekvenc raka na dojki v začetnih stopnjah.